RSC Advances

PAPER

View Article Online
View Journal | View Issue

Cite this: *RSC Adv.*, 2025, **15**, 28248

Preparation and mechanism of environmentally friendly poly-citrulline as shale inhibitor for water-based drilling fluids

Baojun Li,[ac] Pingya Luo,*[a] Danchao Huang,*[ab] Qiang Fu,[c] Leichuan Tan,[c] Xiangyang Zhao,[c] Wei Yan,[b] Shilin Chen,[b] Yuqing Mao[b] and Henry Paul Romero Cortez[d]

Shale inhibitors is a treatment agent in mud, but most inhibitors cannot balance the relationship between inhibition performance and environmental protection performance. In this paper, poly-citrulline was synthesized using citrulline. Fourier transform infrared spectroscopy, gel permeation chromatography, thermogravimetric analysis and toxicity tests were used to characterize the PCCP, and linear expansion tests, rolling recovery tests and sodium bentonite dispersion tests were utilized to measure the inhibitory performance of the PCCP. Its mechanism of action was studied through zeta potential tests, X-ray diffraction and laser particle size. The experimental results revealed that PCCP is a low-molecular-weight nontoxic polymer with excellent inhibitory properties. When 1.5 wt% PCCP was added, the linear expansion rate was 26.4%, the rolling recovery rate was 78.4%, and the Na-Bent dispersion was inhibited by 16%. PCCP is adsorbed on clay particles, compressing the electric double layer and reducing the negative charge. At the same time, the molecules are partially intercalated into the crystal layer space of the clay but more so by wrapping the clay particles, hindering the water molecules from contacting the clay particles and inhibiting the hydration and dispersion of the clay minerals. This article provides environmentally friendly and efficient design ideas for shale inhibitors.

Received 4th June 2025
Accepted 17th July 2025

DOI: 10.1039/d5ra03965g

rsc.li/rsc-advances

1 Introduction

In an era of rapid development within the petroleum and natural gas sector, shale gas is being extracted at an accelerated rate as a clean and efficient energy source, leading to an increasing demand for drilling programs.[1–3] As a key fluid in drilling engineering, mud performs an irreplaceable function in cooling the drill bit, lubricating the drilling tools and carrying the rock cuttings.[4,5] Commonly used drilling fluids are mainly oil-based drilling fluids (OBDFs) and water-based drilling fluids (WBDFs). OBDFs have good lubricating and inhibiting properties, but their application is constrained by rigorous environmental laws and high costs.[6,7] In contrast, WBDFs have are now the favored drilling fluid due to their affordability and environmental benefits.[8–10] However, the employment of WBDFs often leads to expansion and hydration of clay, especially in shale formations. Shale formations account for 75% of the formations drilled, with 90% of the downhole complications occurring in mud shale formations.[11] The hydration of mud shale can easily lead to the instability of the well wall, which in turn can lead to the collapse of the well wall, the shrinkage of the borehole, the card drill and other accidents, resulting in large economic losses and the waste of production time.[12,13] Hence, developing environmentally friendly and effective inhibitors, especially those that inhibit the hydration and swelling of clay minerals,it is vital to formulate WBDFs with efficient inhibition properties.

Over the past fifty years, engineers have attempted to use various chemicals that can inhibit clay minerals hydration expansion as shale inhibitors in WBDFs, aiming to enhance their inhibitory properties and ensure wellbore stability. Before 1990, the inhibitor most commonly in use was KCl, which inhibited hydration expansion by replacing weakly hydrated sodium ions with strongly hydrated potassium ions between clay mineral layers.[14] In most cases, KCl is used in conjunction with other polymers (such as polyethylene glycol) to enhance its inhibitory properties.[15] However, high concentrations of KCl cause serious harm to ecosystems and adversely affect other polymer treatment agents in drilling fluids.[16,17] To overcome the shortcomings of KCl inhibitors, engineers continue to look for alternatives. Organic inhibitors such as quaternary ammonium salts, poly-etheramines, and asphalt have been developed and

[a]*Country State Key Laboratory of Oil and Gas Reservoir Geology and Exploitation, School of Oil & Natural Gas Engineering, Southwest Petroleum University, Chengdu 610500, China. E-mail: luopy@swpu.edu.cn; 202099010153@swpu.edu.cn*
[b]*College of Chemistry and Chemical Engineering, Southwest Petroleum University, Chengdu 610500, PR China*
[c]*CNPC Chuanqing Drilling Engineering Company Limited, Chengdu 610056, China*
[d]*Central University of Ecuador Quito, 170520, Ecuador*

applied.[18–20] The use of organic inhibitors has been acknowledged as crucial to ecosystem development. However, some organic inhibitors may have adverse ecological effects, *e.g.*, ammonium salts decompose readily into ammonia.[21] With the increasingly stringent requirements of environmental protection policies, it is particularly important to balance the inhibitory properties of inhibitors with environmental protection.

In recent years, several environmentally friendly materials, such as ionic liquids, nanomaterials, natural plant extracts and graphene, have been investigated as shale inhibitors.[22–26] Amino acids are natural plant extracts that are polymerized to obtain an important functional polymer (polyamino acid). Polyamino acids are commonly employed in the food, medical, agricultural and engineering sectors.[27] Citrulline is an α -amino acid with hydrophobic carbon chains and amino groups and other functional groups, and is widely present in various melons, vegetables and fruits. Moreover, it has a relatively high level of safety and is beneficial to the human body when consumed in moderation. Poly-citrulline is a polymer composed of citrulline that has been used in the food industry.[28] Due to its advantages such as simple synthesis method, degradability, low toxicity, long hydrophobic carbon chain and large amount of amino groups, it has the potential to be used as a shale inhibitor.

In this paper, polycitrulline (PCCP) was prepared through thermal polymerization as a high-performance, environmentally friendly shale inhibitor. Its inhibitory performance was systematically evaluated through linear expansion tests, shale rolling recovery tests and sodium bentonite (Na-Bent) dispersion tests. In addition, the inhibition mechanism of PCCP was studied by zeta potential tests, X-ray diffraction tests and laser particle size analysis tests. Then, the toxicity of PCCP was studied through biological toxicity tests. Finally, it is expected to obtain an inhibitor PCCP with low toxicity, large molecular weight and good inhibitory effect, and it is hoped that this study can provide valuable references for the preparation of environmentally friendly high-performance shale inhibitors.

2 Materials and methods

2.1 Materials

Sodium bentonite (Na-Bent) was purchased from Bohai Drilling Engineering Co., Ltd (CNPC) Mud Technology Service Branch. Sodium montmorillonite with 98% was sourced from Nanocor (USA). Shale cuttings were collected from an oil field in the Sichuan Basin (China). Analytical pure citrulline (CCP) and sodium hydroxide were obtained from MICXY (Chengdu, China).

2.2 Synthesis of the PCCP

A 40 wt% sodium hydroxide solution was prepared by dissolving 2.0 g of sodium hydroxide in 3.0 g of deionized water. Citrulline (5.0 g) and sodium hydroxide solution (1.5 g) were mixed in a crucible and stirred for 1 h. The mixture was then heated in a muffle furnace at 220 °C for 4 h and stirred every 1 h. Poly-citrulline (PCCP) was obtained by dialysis. The synthesis route is shown in Scheme 1.

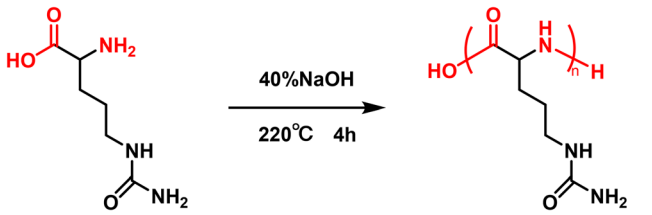

Scheme 1 Synthesis of PCCP.

2.3 Characterization of PCCP

2.3.1 Fourier transform infrared (FTIR) spectroscopy test. FT-IR of the products was performed on a Thermo Scientific, Nicolet iS50 spectrometer. PCCP and KBr powder were mixed with the mass ratio of 1 : 100, and a flake was prepared by pressing method, then put into the infrared spectrometer for testing the functional groups. The range was from 4000 cm^{-1} to 400 cm^{-1} with a resolution of 2 cm^{-1}.

2.3.2 Gel permeation chromatography (GPC) test. The weight average molecular weight (M_w) of PCCP was measured with GPC, using a mobile phase of 0.1 mol L^{-1} $NaNO_3$ and 0.05% NaN_3, at a flow rate of 0.6 mL min^{-1} and a temperature of 35 °C, with calibrated against narrow distribution polyethylene glycol.

2.3.3 Thermogravimetric analysis (TGA) test. The thermogravimetric curve of PCCP was obtained using a TGA (Mettler Toledo TGA 2 STARe). A 10 mL min^{-1} nitrogen atmosphere was used for protection, and heat samples from 30 °C to 800 °C at 15 °C min^{-1}.

2.3.4 Biological toxicity (EC50) test. A 1.0 wt% PCCP solution was diluted with 3 wt% NaCl to various concentrations. The experimental and control groups were tested for EC_{50} using a luminescent bacterial assay.[6] The relative luminescence of the sample was obtained using formula (1).[6] Formula (2) was used to calculate the EC_{50} number of each sample. When the EC_{50} value is greater than 25 000, indicating that the test sample is non-toxic.

$$T = E_1/E_2 \times 100 \quad (1)$$

where T is the relative luminosity (%), E_1 is the luminous intensity of the experimental group, and E_2 is the luminous intensity of the control group.

$$EC_{50} = C \times 10^8 \quad (2)$$

where C is the concentration of the sample when the relative luminosity is 50% (g mL^{-1}).

2.4 Evaluation of inhibition performance

2.4.1 Linear expansion test. Na-Bent (8.0 g) was compacted under 10 MPa for 5 minutes. Swelling height (L) was measured after 24 hours at different inhibitor concentrations using a NP-2S dual-channel dilatometer (Tongchun, Qingdao, China), and linear expansion rate was calculated using formula (3) (Huang *et al.*, 2020).

$$W = L/H \times 100\% \quad (3)$$

where W is the linear expansion rate (%), H is the height of the Na-Bent core (mm), and L is the swelling height (mm).

2.4.2 Rolling recovery test. Large shale blocks are crushed to obtain shale cuttings with a size of 6 to 10 mesh, which are dried at 105 °C.Shale cuttings (50.00 g) were mixed with 350 mL of inhibitor solution at different concentrations and aged at 150 °C for 16 hours. The recovered shale cuttings were obtained by screening the shale using a 40-mesh screen and slowly rinsing it with clean water. The recovered shale cuttings are then dried and weighed at 105 °C to determine the rolling recovery rate (R) using formula (4).

$$R = M/50 \times 100\% \quad (4)$$

where R is the rolling recovery rate of the shale cuttings (%), and M is the recovery mass (g).

2.4.3 Na-Bent dispersion test. Na-Bent (12.0 g) was dispersed in 300 mL of deionized water or inhibitor solutions and stirred for 30 minutes. Rheological parameters were recorded with a ZNN-D6L six-speed rotary viscometer, and dynamic shear force (YP) was calculated using eqn (5)–(7). Then, 12.0 g of Na-Bent was added, and the above steps were repeated until the inflection point occurred.

$$AV = \theta_{600}/2 \quad (5)$$

$$PV = \theta_{600} - \theta_{300} \quad (6)$$

$$YP = AV - PV \quad (7)$$

2.5 Inhibition mechanism analysis

2.5.1 Laser particle size test. The particle size distribution of the 4 wt% Na-Bent dispersion was determined using a Malvern Mastersizer 2000. Before the tests, the suspension needs to be ultrasonic dispersed for 5 min.

2.5.2 X-ray diffraction test. 50 mL inhibitor solution of different concentrations was prepared, 1.0 g of Na-MMT was added, and the mixture was stirred for 1 h, followed by centrifugation at 5000 rpm for 10 min to obtain solid precipitate. X-ray diffraction patterns in the range of 2θ = 3–40° were obtained using an X'Pert Pro MPD diffractometer. The interlayer spacing was determined using Bragg's equation.

2.5.3 Zeta potential test. Sodium montmorillonite was dispersed in deionized water and 4.0 wt% Na-Bent dispersion was prepared using magnetic stirring for 12 h. The sodium montmorillonite dispersion was then mixed with 2.0 wt% inhibitor and vigorously stirred for 12 h. The supernatant of the dispersion was diluted and loaded into the sample cell of a dynamic light scattering instrument (Zeta PALS 190 Plus) and measurement parameters were set for characterization.

3 Results and discussion

3.1 Characterization of PCCP

3.1.1 Fourier transform infrared spectroscopy test. FTIR is used to analyse chemical bonds in compounds to determine their molecular structure (Smith, 2011). Fig. 1 shows the FTIR spectrum of the PCCP. The characteristic peak at 3430 cm^{-1} responds to the O–H stretching vibration in the amino group and hydroxyl group, the characteristic peak at 1627 cm^{-1} corresponds to the C=O stretching vibration in the urea group and amide, and the characteristic peak at 1594 cm^{-1} corresponds to the N–H bending vibration in the amide. The characteristic peak at 1350 cm^{-1} corresponds to the C–H in-plane bending vibration in the methylene group, and the characteristic peak at 1117 cm^{-1} corresponds to the C–C stretching vibration in the methylene group(Smith, 2011). According to the experimental results, PCCP was successfully prepared.

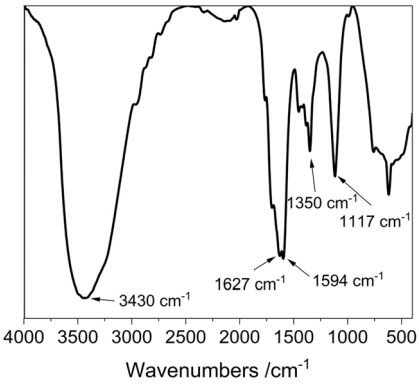

Fig. 1 Infrared spectrum of the PCCP.

Table 1 GPC test results for the PCCP

Sample	Weight-average molecular weight
PCCP	984

3.1.2 Gel permeation chromatography test. Table 1 shows the GPC results for the PCCP. the weight average molecular weight of PCCP is 984, indicating that PCCP is between large molecules and small molecules.

3.1.3 Thermogravimetric analysis test. Thermogravimetric analysis is used to evaluate changes in the weight of materials due to temperature changes. Fig. 2 reveals the

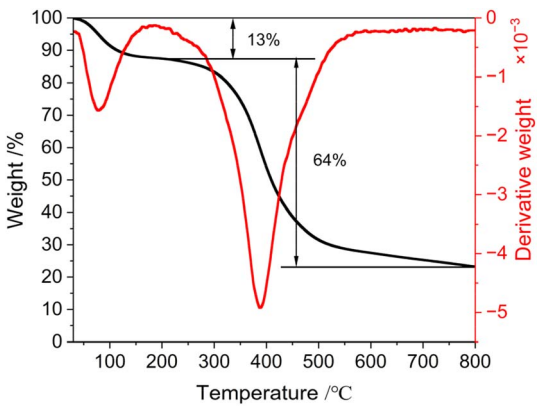

Fig. 2 Thermogravimetric curve of the PCCP.

thermogravimetric analysis curve of the PCCP. The first degradation observed in the temperature range of 30–200 °C can be attributed to the volatilization of free water, resulting in a mass loss of approximately 13% for PCCP. The second degradation phase occurs between 200 and 800 °C with a 64% mass loss, probably due to the decomposition of the PCCP sample. The experimental results show that PCCP has a good thermal stability to minimize the interaction between shale and water during drilling.

3.1.4 Biological toxicity test. Fig. 3 shows the PCCP sample concentration as a function of the relative luminescence intensity. As calculated through formula (5), the concentration of the PCCP solution when the relative luminescence intensity was 50% was 0.00062 g mL^{-1}, and the EC_{50} value was 62 000. This value is greater than 25 000 where the PCCP is nontoxic.

3.2 Evaluation of inhibition performance

3.2.1 Linear expansion test. The linear expansion test is a method used to measure an inhibition of the hydrological swelling of clay.[29] Fig. 4 illustrated the swelling of Na-Bent in PCCP solutions at various concentrations. The swelling rate of the blank group sample at 24 h was 38.6%, demonstrating the strong hydration potential of Na-Bent. With the addition of 0.5 wt% PCCP, the linear expansion rate decreased to 34.4%, indicating that PCCP has the ability to inhibit the hydration of Na-Bent. As the PCCP concentration increases, the inhibitory performance gradually increases. Increasing the PCCP concentration to 1.5 wt% results in a linear expansion rate of 26.4%, with only a minor further decrease, indicating that the inhibitory effect of 1.5 wt% PCCP tended to be optimal. The experimental results show that 1.5 wt% PCCP has a good capacity to inhibit the hydration of clay minerals.

3.2.2 Rolling recycling test. The rolling recovery experiment is a common method for evaluating the inhibition performance by measuring the hydration and dispersion of shale cuttings.[30] Fig. 5 shows the recovery rate of shale cuttings in PCCP solutions with various concentrations. The recovery rate of the blank group sample is 33.4%, indicating that the cuttings are standard cuttings for shale rolling recovery experiments. With the addition of 0.5 wt% PCCP, the rolling recovery rate increased to 51.3%, indicating that PCCP can prevent the dispersion of cuttings. As the concentration increases, the ability of PCCP in inhibiting the of cuttings increases. When the PCCP concentration was increased to 1.5 wt%, the rolling recovery was 78.4%, indicating that PCCP had good inhibition properties. When the concentration was further increased to 2.0 wt%, the rolling recovery was only increased by 2.5%. Given the relatively limited performance gain from increasing the inhibitor concentration, combined with cost factors, 1.5 wt% was determined to be the optimal concentration for PCCP application.

3.2.3 Na-Bent dispersion test. The Na-Bent dispersion experiment was used to assess the effectiveness of shale inhibitors in preventing the hydration and dispersion of Na-Bent. The dynamic shear force of WBDFs reflects the strength of the internal network structure created by dispersed Na-Bent particles under laminar flow. The greater the dynamic shear force is, the greater the number of dispersed particles and the stronger the network structure. Fig. 6 shows the dynamic shear force of the Na-Bent/PCCP dispersion. The degree of dispersion of Na-Bent is affected by the PCCP concentration. Since the amount of PCCP adsorbed on Na-Bent particles is smaller, the

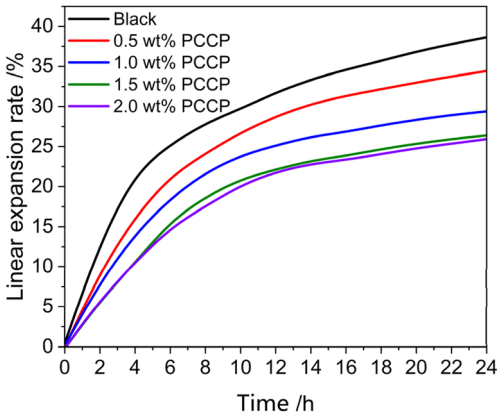

Fig. 4 Linear expansion rate of Na-Bent in PCCP solutions with different concentrations.

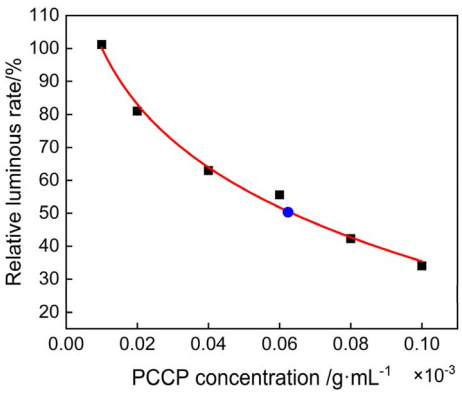

Fig. 3 Biological toxicity of PCCPs.

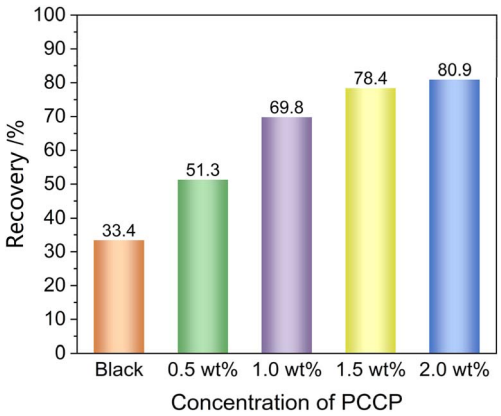

Fig. 5 Rolling recovery rate of shale cuttings in PCCP solutions with different concentrations.

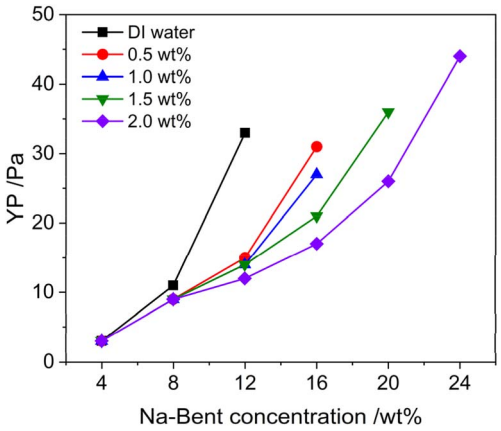

Fig. 6 Relationship between the dynamic shear force of the Na-Bent/PCCP suspension and the Na-Bent concentration.

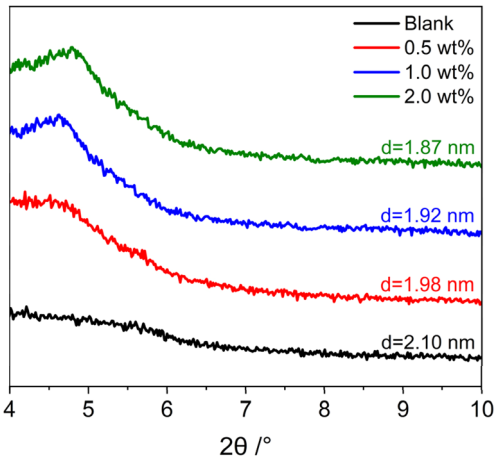

Fig. 8 X-ray diffraction pattern of Na-MMT/PCCP.

degree of dispersion in lower concentration solutions is greater than that in higher concentration solutions. As the Na-Bent concentration increases, the dynamic shear forces of all the samples increase, and the gap between the dynamic shear forces gradually increases.

In deionized water, Na-Bent disperses better, as manifested by greater dynamic shear forces at low Na-Bent concentrations. In the inhibitor solution, under low Na-Bent concentration conditions, only a small amount of PCCP molecules can undergo saturated adsorption on Na-Bent, resulting in similar inhibitory properties of PCCP at different concentrations. However, at relatively high Na-Bent concentrations, a smaller number of PCCP molecules are available for adsorption onto Na-Bent, resulting in a more pronounced inhibitory effect in samples with high PCCP concentrations.

3.3 Inhibition mechanism analysis

3.3.1 Zeta potential. Zeta potential studies were employed to analyse the effects of the inhibitors on the stability of the system. As the absolute value of the zeta potential decrease, the system become more unstable. Fig. 7 shows the zeta potential of Na-Bent after treatment with the inhibitors. In the blank group, Na-Bent was completely hydrated and dispersed, and the zeta potential was −53 mV, indicating that Na-Bent has a characteristic negative charge and significant stability. The addition of inhibitors led to an increase in zeta potential values, indicating that the inhibitors adsorbed on the surface of the Na-Bent particles, compressed the diffusion double electric layer, reduced the repulsive force between the particles, and made the dispersion less stable. The zeta potential values of 2wt%KCl, 2wt%HIH, and 2wt%PCCP are −41 mV, −25 mV, and −20 mV, respectively, indicating that the ability to compress the diffusion double electric was in order of PCCP > HIH > KCl from the strongest to the weakest.

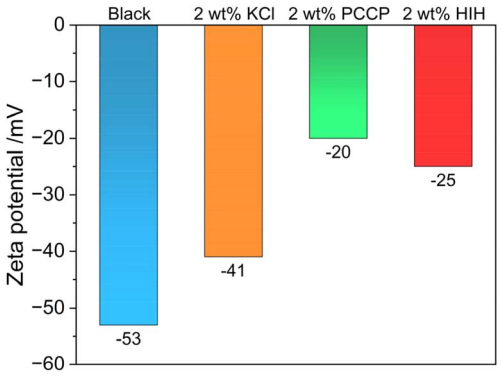

Fig. 7 Zeta potential of Na-Bent/inhibitor under different inhibitor conditions.

3.3.2 X-ray diffraction test. The mechanism of PCCP was analysed by studying the changes in the interlayer spacing of Na-MMT with X-ray diffraction. Fig. 8 shows that the interlayer spacing of the fully hydrated and dispersed Na-MMT in the blank group sample was 2.10 nm. When PCCP is added, the interlayer spacing of Na-MMT decreases, indicating that PCCP may enter the intercalation space of Na-MMT and reduce the interlayer spacing to inhibit hydration and dispersion. As the amount of PCCP increases from 0.5 wt% to 2.0 wt%, the interlayer spacing of Na-MMT decreases from only 1.98 nm to 1.87 nm, indicating that reducing the interlayer spacing through intercalation does not main effect of inhibiting the hydration and dispersion of clay mineral. According to the experimental data, PCCP does not inhibit the hydration and dispersion of clay minerals through intercalation but may inhibit their hydration and dispersion by wrapping clay minerals. Laser particle size analysis was further employed to study the particle size distribution of Na-MMT/PCCP.

3.3.3 Laser particle size test. Na-Bent forms fine particles after being hydrated and dispersed in water. By studying the changes in Na-Bent particle size after the addition of the inhibitor, we analyse the inhibition mechanism of the inhibitor. Table 2 shows the D50 values after adding different inhibitors. Fig. 9 shows the particle size distribution of Na-Bent under the action of different inhibitors.

Table 2 D_{50} values of Na-Bent under different inhibitor conditions

	D_{50}/um
Black	8.016
2 wt% KCl	8.430
2 wt% HIH	14.560
2 wt% PCCP	49.320

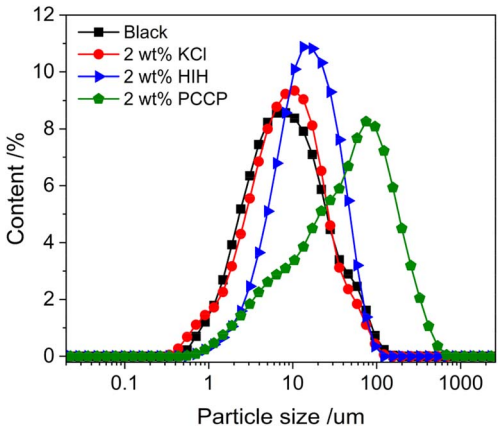

Fig. 9 Particle size distribution of Na-Bent under different inhibitor conditions.

In the blank group sample, Na-Bent hydrated and dispersed to form a suspension with a D50 of 8.016 μm. Adding 2 wt% KCl had no obvious effect on the size of the Na-Bent particles, with D_{50} being 8.430 μm. This is because KCl inhibits its hydration and dispersion by replacing the strongly hydrated sodium ions in Na-Bent with weakly hydrated potassium ions. With the addition of 2 wt% HIH (Hydrophobic inhibitors) and 2 wt% PCCP, the particle size of Na-Bent increased significantly, and that of D_{50} increased to 14.560 μm and 49.320 μm, respectively, indicating that the inhibitor encapsulates Na-Bent to prevent hydration and dispersion.

Firstly, the surface of PCCP has positively charged amino groups, which can be electrostatically adsorbed onto the negatively charged surface of shale. Moreover, its hydrophobic carbon chains can form a dense hydrophobic layer on the surface of clay minerals, preventing water molecules from approaching the clay and thereby reducing the driving force for surface hydration. Zata potential measurement indicates that PCCP adsorbs on the surface of clay minerals, compresses the double electric layer around the clay minerals, and increases the zeta potential of Na-Bent.

Secondly, the XRD experiments indicated that some PCCP molecules were inserted into the crystal layer spaces between the clay minerals, slightly reducing the crystal layer spacing. Finally, laser particle size analysis indicated that more PCCP molecules were adsorbed on the surface of clay minerals, bridging and encapsulating the clay minerals, increasing the particle size of Na-Bent, thereby effectively inhibiting the hydration expansion of clay minerals.

4 Conclusion

It is important to balance the inhibitory properties and environmental protection of shale inhibitors. Organic inhibitors have excellent inhibitory properties, but most of them are toxic compounds and cannot be discharged directly. In this article, an environmentally friendly PCCP was prepared as a shale inhibitor, and the following conclusions were obtained:

(1) At a concentration of 1.5 wt%, the linear expansion rate of PCCP was only 26.4%. Under conditions of 150 °C, its rolling recovery reached 78.4%, suggesting that it is more effective in inhibiting the hydration swelling of clay minerals and is suitable for use as a shale inhibitor in water-based drilling fluids.

(2) Based on our inhibition mechanism analysis, we elucidated the inhibition mechanism of PCCP. The surface of PCCP has a positively charged amino group, which can have electrostatic interaction with negatively charged sodium montmorillonite. The zata potential indicates that PCCP compresses the diffusion electric double layer and adsorbs on the surface of sodium montmorillonite. At the same time, the XRD results showed that a part of the PCCP intercalation entered sodium montmorillonite. Moreover, the zata potential showed that PCCP encapsulated sodium montmorillonite particles and prevented the invasion of water molecules, thereby successfully inhibiting the hydration and dispersion of clay minerals.

At present, this paper only focuses on the direct polymerization of amino acids to prepare polyamino acid compounds, and the next step will be to carry out the modification of amino acids and then polymerization to enhance the inhibitory properties of polyamino acids and reduce the dosage of polyamino acids. This study offers a valuable reference for the preparation of environmentally friendly high-performance shale inhibitors.

Data availability

The datasets supporting this study, including raw data from FTIR, GPC, TGA, zeta potential, XRD, particle size analysis, and all inhibition performance tests (linear expansion, rolling recovery, and dispersion tests), are available from the corresponding author upon reasonable request.

Conflicts of interest

No potential conflict of interest was reported by the author(s).

Acknowledgements

We would like to thank the Financial Support of the National Natural Science Foundation of China (No. 52404010).[12]

References

1 L. Dou, Z. Wen, J. Wang, Z. Wang, Z. He, X. Liu, *et al.*, Analysis of the world oil and gas exploration situation in 2021, *Pet. Explor. Dev.*, 2022, **49**(5), 1195–1209.
2 Z. He, Y. Yang, J. Qi, X. Lin, N. Wang, L. Wang, *et al.*, Hyperbranched polymer nanocomposite as a potential

shale stabilizer in water-based drilling fluids for improving wellbore stability, *J. Mol. Liq.*, 2024, **395**, 123903.

3 J. Jin, K. Lv, J. Sun, J. Zhang, Q. Hou, X. Guo, *et al.*, Robust superhydrophobic TiO_2@carbon nanotubes inhibitor with bombax structure for strengthening wellbore in water-based drilling fluid, *J. Mol. Liq.*, 2023, **370**, 120946.

4 S. Gautam, C. Guria and V. K. Rajak, A state of the art review on the performance of high-pressure and high-temperature drilling fluids: Towards understanding the structure-property relationship of drilling fluid additives, *J. Pet. Sci. Eng.*, 2022, 213.

5 J. Guancheng, D. Tengfei, C. U. I. Kaixiao, H. E. Yinbo, Q. Xiaohu, Y. Lili, *et al.*, Research status and development directions of intelligent drilling fluid technologies, *Pet. Explor. Dev.*, 2022, **49**(3), 660–670.

6 S. Chen, D. Huang, Z. Xu, Y. Bai, G. Xie, X. Li, *et al.*, Synthesis and mechanism analysis of a non-toxic amine-based clay mineral surface hydration intercalation inhibitor, *J. Mol. Liq.*, 2024, 399.

7 J.-S. Sun, Z.-L. Wang, J.-P. Liu, K.-H. Lv, F. Zhang, Z.-H. Shao, *et al.*, Notoginsenoside as an environmentally friendly shale inhibitor in water-based drilling fluid, *Pet. Sci.*, 2022, **19**(2), 608–618.

8 G. Jiang, J. Sun, Y. He, K. Cui, T. Dong, L. Yang, *et al.*, Novel Water-Based Drilling and Completion Fluid Technology to Improve Wellbore Quality During Drilling and Protect Unconventional Reservoirs, *Engineering*, 2022, **18**, 129–142.

9 J. Li, Z. Qiu, H. Zhong, X. Zhao, Z. Liu and W. Huang, Effects of water-based drilling fluid on properties of mud cake and wellbore stability, *J. Pet. Sci. Eng.*, 2022, **208**, 109704.

10 M. Murtaza, H. M. Ahmad, X. Zhou, D. Al-Shehri, M. Mahmoud and M. S. Kamal, Okra mucilage as environment friendly and non-toxic shale swelling inhibitor in water based drilling fluids, *Fuel*, 2022, **320**, 123868.

11 F. Zhang, J. Sun, Q. Li, K. Lv, J. Wang and Z. Wang, Mechanism of organosilicate polymer as high-temperature resistant inhibitor in water-based drilling fluids, *Colloids Surf., A*, 2022, **641**, 128489.

12 M. A. Abbas, A. Zamir, K. A. Elraies, S. M. Mahmood and M. H. Rasool, A critical parametric review of polymers as shale inhibitors in water-based drilling fluids, *J. Pet. Sci. Eng.*, 2021, **204**, 108745.

13 D. Huang, X. Li, Y. Bai, G. Xie, S. Chen, H. Chen, *et al.*, Structure-activity relationships for hydration inhibition and environmental protection with modified branched polyethyleneimine: Experiments and simulations, *Energy*, 2023, **284**, 129346.

14 N. S. Muhammed, T. Olayiwola, S. Elkatatny, B. Haq and S. Patil, Insights into the application of surfactants and nanomaterials as shale inhibitors for water-based drilling fluid: a review, *J. Nat. Gas Sci. Eng.*, 2021, **92**, 103987.

15 D.-C. Huang, G. Xie, N.-Y. Peng, J.-G. Zou, Y. Xu, M.-Y. Deng, *et al.*, Synergistic inhibition of polyethylene glycol and potassium chloride in water-based drilling fluids, *Pet. Sci.*, 2021, **18**(3), 827–838.

16 L. Fu, K. Liao, J. Ge, Y. He, W. Huang and E. Du, Preparation and inhibition mechanism of bis-quaternary ammonium salt as shale inhibitor used in shale hydrocarbon production, *J. Mol. Liq.*, 2020, **309**, 113244.

17 D. Huang, G. Xie, P. Luo, M. Deng and J. Wang, Synthesis and mechanism research of a new low molecular weight shale inhibitor on swelling of sodium montmorillonite, *Energy Sci. Eng.*, 2020, **8**(5), 1501–1509.

18 H. Zhong, Z. Qiu, D. Sun, D. Zhang and W. Huang, Inhibitive properties comparison of different polyetheramines in water-based drilling fluid, *J. Nat. Gas Sci. Eng.*, 2015, **26**, 99–107.

19 N. S. Muhammed, T. Olayiwola and S. Elkatatny, A review on clay chemistry, characterization and shale inhibitors for water-based drilling fluids, *J. Pet. Sci. Eng.*, 2021, **206**, 109043.

20 C. Zhang, K. Lv, J. Gong, Z. Wang, X. Huang, J. Sun, *et al.*, Synthesis of a hydrophobic quaternary ammonium salt as a shale inhibitor for water-based drilling fluids and determination of the inhibition mechanism, *J. Mol. Liq.*, 2022, **362**, 119474.

21 J. Ma, B. Xia and Y. An, Advanced developments in low-toxic and environmentally friendly shale inhibitor: a review, *J. Pet. Sci. Eng.*, 2022, **208**, 109578.

22 H. Ao, L. Lin, R. Ren, Y. Yang, X. Li, W. Ren, *et al.*, Deep Eutectic Solvents with Different Alkyl Chain Lengths as Inhibitors for Shale in Water-Based Drilling Fluids, *Energy Fuels*, 2024, **38**(6), 5374–5380.

23 X. Li, G. Jiang, J. Wang and X. Ni, Inhibitive properties comparison of different polyamino acids in water-based drilling fluids, *J. Nat. Gas Sci. Eng.*, 2020, **83**, 103589.

24 S. MT-u, B. R. Pandian, N. E. A. Kahar and M. N. M. Ibrahim, Mechanical exfoliation of coconut husk into bio-based graphene for sustainable drilling mud: a Taguchi-GRA Study, *Carbon Lett.*, 2025, DOI: **10.1007/s42823-025-00938-y**.

25 J.-J. Dai, K.-H. Lv, J.-S. Sun, H. Jia, X.-B. Huang and J. Li, Exploring the synergistic effects and mechanistic insights of ionic and polyionic liquid combinations as shale inhibitors, *Pet. Sci.*, 2025, **22**(4), 1566–1577.

26 W. Qin, Y. Li, Y. An, M. Wang and M. Guo, Silicate nanoemulsion for high-temperature wellbore stabilization *via* hydrophobic sealing and nano-pore plugging, *Colloids Surf., A*, 2025, 724.

27 G. Carrea, S. Colonna, D. R. Kelly, A. Lazcano, G. Ottolina and S. M. Roberts, Polyamino acids as synthetic enzymes: mechanism, applications and relevance to prebiotic catalysis, *Trends Biotechnol.*, 2005, **23**(10), 507–513.

28 X. Ma, H. Lv, Q. Zhu, M. Chen, Y. Wang and F. Li, A novel sensitive electrochemical method for the detection of ractopamine in meat food *via* polycitrulline-modified electrode, *Food Addit. Contam. Part A, Chem. Anal. Control Expo. Risk Assess.* , 2020, **37**(9), 1459–1466.

29 Q. Chu, L. Lin and J. Su, Amidocyanogen silanol as a high-temperature-resistant shale inhibitor in water-based drilling fluid, *Appl. Clay Sci.*, 2020, **184**, 105396.

30 J. Liu, Y. Li, K. Lv, J. Sun, Z. Li, L. Dai, *et al.*, Shrimp Shell-Derived Chitin Nanofibers as Shale Inhibitors in Water-Based Drilling Fluids, *ACS Sustainable Chem. Eng.*, 2024, **12**(30), 11130–11144.